Synthesis and Characterization of $CeCu_2Si_{2-x}P_x$

S. M. Saunders[1,2], A. Gallagher[2], Y. Lai[2], K.-W. Chen[2], S.-Z. Zhang[2], D. Graf[2] and R. E. Baumbach[2]

[1]*Department of Physics and Astronomy – Iowa State University*

[2]*National High Magnetic Field Laboratory – Florida State University*

Introduction

Correlated d- and f-electron materials that evade description in terms of localized or itinerant pictures remain at the forefront of condensed matter physics, owing both to the difficulties that they present to theory and the fascinating behavior that they often exhibit: e.g., unconventional superconductivity, non-Fermi-liquid behavior, nematic fluctuations, etc. The heavy fermion superconductor, $CeCu_2Si_2$, is a well known example and although its discovery pre-dates that of the cuprates **[1,2]**, it continues to attract attention. Like many other correlated electron superconductors, $CeCu_2Si_2$ is located in the vicinity of an antiferromagnetic quantum critical point, where magnetic fluctuations may provide the "glue" for superconductivity **[3]**. Surprisingly, a second dome of superconductivity is seen in the chemical substitution series $CeCu_2Si_{2-x}Ge_x$ under applied pressure, where the superconductivity is not associated with the zero temperature termination of any obvious magnetic or structural phase transition **[4]**. This behavior has led to speculation that a Ce valence quantum phase transition produces the unexpected superconducting dome, indicating the importance of the Ce electronic state **[5,6]**.

To gain further insight into $CeCu_2Si_2$, we performed a detailed study of the new chemical substitution series $CeCu_2Si_{2-x}P_x$ for $x \leq 0.2$. Ligand site substitution using phosphorous slightly reduces the unit cell volume and results in charge doping. While superconductivity is rapidly destroyed, antiferromagnetism appears at low x. This result is consistent with the view that $CeCu_2Si_2$ is near an antiferromagnetic quantum critical point. At larger x, we unexpectedly find that ferromagnetism appears at low temperatures.

Experimental Methods

Single crystals of $CeCu_2Si_{2-x}P_x$ were grown from elements with purities > 99.9% by a self-flux growth technique. Elements were placed into an alumina crucible in a ratio Ce:Cu:Si:P of 1:28:11.44-x:x respectively for each of the different nominal dopings of P. The alumina crucible was then sealed under a partial argon atmosphere in a quartz silica ampoule and heated to 600°C at a rate of 50°C/hour, held at 600°C for 6 hours, heated to 1185°C at a rate of 50°C/hour, held at 1185°C for 12 hours, and then cooled at a rate of 2°C/hour to 940°C. At this point, the remaining flux was separated from the crystals by centrifuging.

Phosphorous concentrations were obtained using energy dispersive spectroscopy (EDS). The lattice constants were measured using powder X-ray diffraction. Electrical resistivity ρ and magnetic susceptibility χ were measured using a Quantum Design Physical Property Measurement System (PPMS) and a Magnetic Property Measurement System (MPMS), respectively.

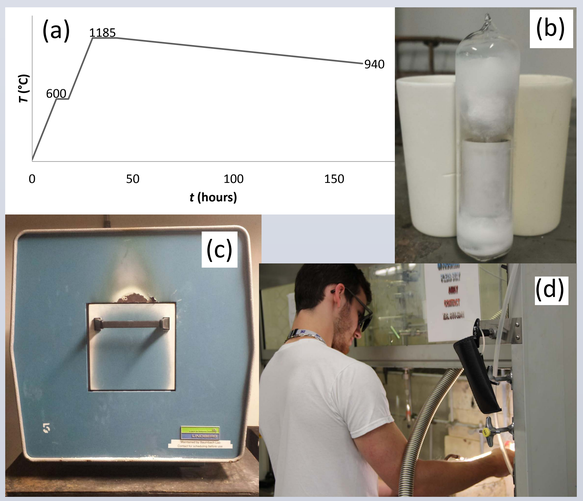

FIG. 1. (a) Schematic heating profile for $CeCu_2Si_{2-x}P_x$, (b) Sealed quartz ampoule with elements contained in alumina crucible, (c) Box furnace, (d) the Undergrad in his natural habitat

$CeCu_2Si_{2-x}P_x$ Crystal Structure

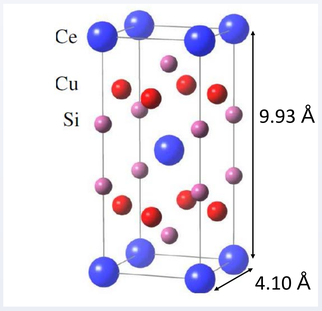

FIG. 2. $CeCu_2Si_2$ crystalizes in the tetragonal $ThCr_2Si_2$ prototype (space group I4/*mmm*) **[7]**. This structure is characterized by square lattices of Ce ions that are separated by corrugated Cu/Si layers.

P substitution: lattice constants

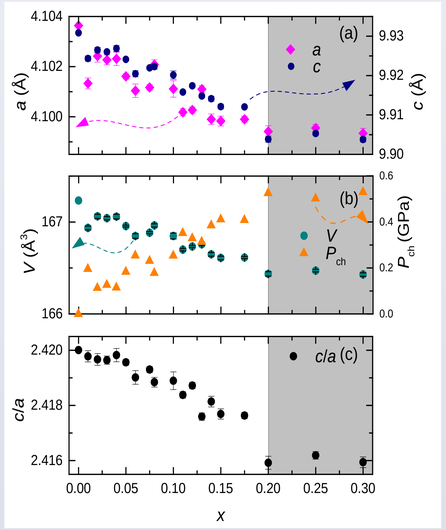

FIG. 3. (a) The lattice constants, $a(x)$ (left axis) and $c(x)$ (right axis), (b) the unit cell volume $V(x)$ (left axis) and chemical pressure P_{ch} (right axis), and (c) the ratio c/a vs. x. These lattice constants were obtained from powder X-ray diffraction measurements. P_{ch} was determined by calculating $\Delta V(x)/V(0)$ and multiplying by the Bulk Modulus (110 GPa) **[8]**.The grayed out region represents the region beyond which the P concentration saturates .

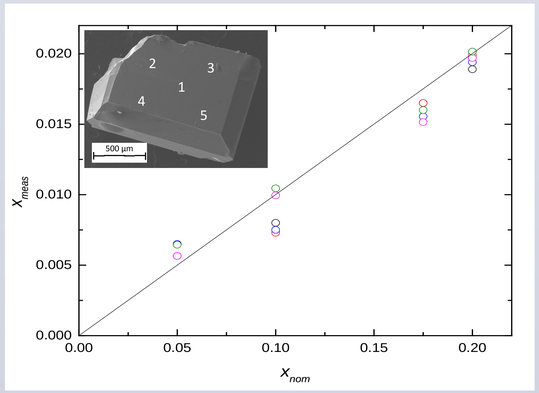

FIG. 4. x-values obtained through P doping acquired using energy dispersive spectroscopy (EDS) for $CeCu_2Si_{2-x}P_x$. Samples with different initial P doping values were measured (x_{nom}). EDS measurements were made on each sample in several different regions, as shown in the inset. The results of the measurements are plotted vs. nominal P doping.

Magnetic Susceptibility and Resistivity

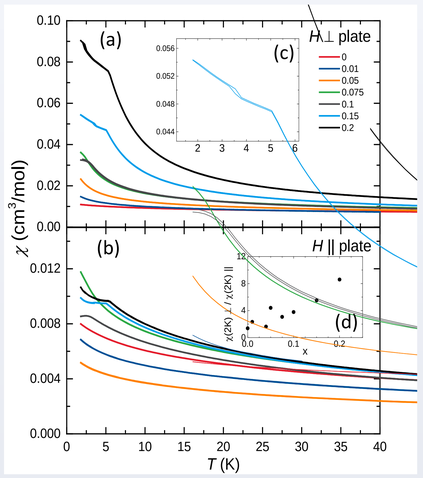

FIG. 5. (a) The magnetic susceptibility $\chi = M/H$ vs. temperature T for $CeCu_2Si_{2-x}P_x$ with $H \perp$ to the a-b plane and (b) $H \parallel$ to a-b plane. Data were acquired in a field of 1 kOe; (c) Zoom of 1-6 K for $x = 0.15$ showing hysteresis in χ; (d) χ(2K) with H applied $\perp$ to plate relative to H applied $\parallel$ to plate for different x values

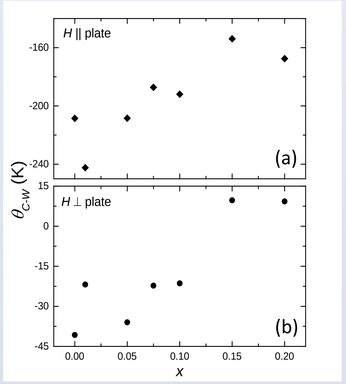

FIG. 6. The Curie-Weiss temperature ($\theta_{C\text{-}W}$) from fits to the magnetic susceptibility data shown in Fig. 5 for various x values with (a) $H \parallel$ to the a-b plane and (b) $H \perp$ to the a-b plane.

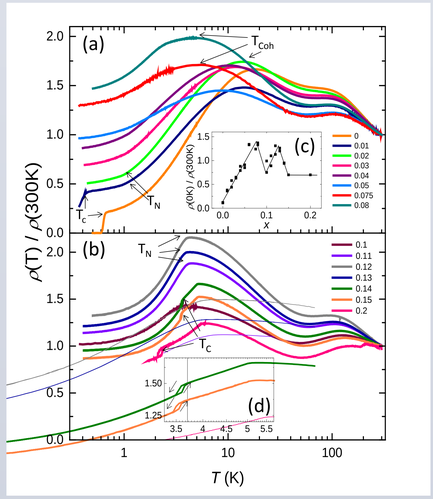

FIG. 7. (a) Electrical resistivity normalized to the value at 300 K ρ/ρ_{300K} vs. temperature T for $CeCu_2Si_{2-x}P_x$ at low x and (b) high x: (c) ρ_{0K}/ρ_{300K} vs. x: (d) Zoom of resistivity showing AFM transition ~ 5 K and hysteretic feature at ~ 3.6 K – arrows represent decreasing and increasing T.

T-x Phase Diagram

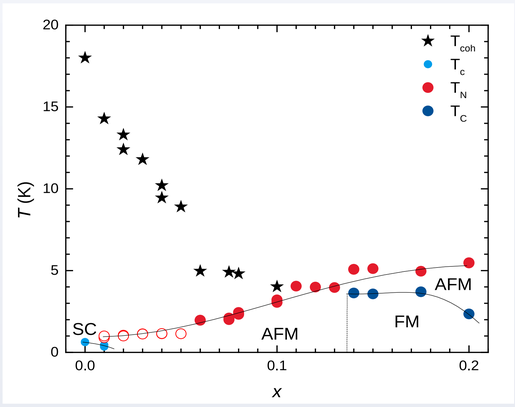

FIG. 8. Temperature T vs phosphorus concentration x phase diagram for $CeCu_2Si_{2-x}P_x$ constructed from magnetic susceptibility χ and electrical resistivity ρ. A dome of superconductivity is present at very low x. Antiferromagnetism appears at low x and persists throughout the doping series. Ferromagnetic behavior abruptly appears for $x = 0.14$ until our system saturates at $x = 0.2$. Open circles represent a broad transition.

Conclusions and Future Work

- New ligand site chemical substitution series in $CeCu_2Si_2$ (Si → P)
- Small chemical pressure effect: the main tuning parameter is variation of the electron count.
- Appearance of Ferromagnetism with a addition of electrons into the system
- Pressure work under way to explore how the addition of electrons effects the system under extreme conditions
- Heat capacity measurements under way to clarify the physical picture behind features seen at various transition temperatures

References

1. Bednorz, J. G. & Muller, K. A. *Z. Phys.* B **1986**, *64*, 189−194
2. F. Steglich *et al. Phys. Rev. Lett.* **1979**, *43*, 1892
3. N. D. Mathur *et al. Nature* **1998**, *394*, 39-43
4. H. Q. Yuan *et al. Science* **2003**, *302*, 2104-2107
5. H. Yamaoka *et al. PRL* **2014**, *113*, 086403
6. F. Steglich *Journal of Physics: Conference Series* **2012,** *400*, 022111
7. G. Knebel *et al. C. R. Physique* **2011**, *12*, 542–566
8. Spain I. L. *et al Physica B* **1986**, *449*, 139–140

Acknowledgements

X-ray Diffraction measurements were performed with equipment in Theo Siegrist's lab. Special thanks to Tiglet Bessara for useful discussion on the operation of equipment and programs. EDS measurements and Scanning Electron Microscopy image were taken with the assistance of Fumitake Kametani at the Applied Superconductivity Center.

Thank you to the National High Magnetic Field Lab (NHMFL) Research Experience for Undergraduates (REU) program for allowing me the opportunity to work with the great scientists and equipment at the NHMFL.

This work was performed at the NHMFL, which is supported by National Science Foundation Cooperative Agreement No. DMR-1157490, the State of Florida and the DOE. A portion of this work was supported by the NHMFL User Collaboration Grant Program (UCGP).